

Fluorescence incoherent color holography

Joseph Rosen* and Gary Brooker

Department of Biology, Integrated Imaging Center, Johns Hopkins University, Montgomery County Campus
Suite 240, 9605 Medical Center Drive, Rockville, MD 20850

*On leave from the Department of Electrical and Computer Engineering, Ben-Gurion University of the Negev,
PO Box 653, Beer-Sheva 84105, Israel.
rosen@ee.bgu.ac.il, gbrooker@jhu.edu

Abstract: We present a new imaging method to record multicolor digital holograms from objects emitting fluorescent light. The fluorescent light specific to the emission wavelength of various fluorescent dyes after excitation of three dimensional (3D) objects is recorded on a digital monochrome camera after reflection from a diffractive optical element (DOE). For each wavelength of fluorescent emission, the camera sequentially records three holograms reflected from the DOE, each with a different phase factor of the DOE's function. The three holograms are superposed in a computer to create a complex valued Fresnel hologram of each fluorescent emission. The holograms for each fluorescent color are further combined in a computer to produce a multicolored fluorescence hologram and 3D color image.

©2007 Optical Society of America

OCIS codes: (050.1950) Diffraction gratings; (070.4550) Optical correlators; (090.0090) Holography; (090.1760) Computer holography; (090.1970) Diffractive optics; (090.2880) Holographic interferometry; (100.6890) Three-dimensional image processing; (110.6880) Three-dimensional image acquisition; (120.5060) Phase modulation; (260.2510) Fluorescence; (330.1720) Color vision

References and links

1. J. Garcia-Sucerquia, W. Xu, S. K. Jericho, P. Klages, M. H. Jericho, and H. J. Kreuzer, "Digital in-line holographic microscopy," *Appl. Opt.* **45**, 836-850 (2006).
2. B. W. Schilling, T.-C. Poon, G. Indebetouw, B. Storrie, K. Shinoda, Y. Suzuki, and M. H. Wu "Three-dimensional holographic fluorescence microscopy" *Opt. Lett.* **22**, 1506-1508 (1997).
3. G. Indebetouw and W. W. Zhong, "Scanning holographic microscopy of three-dimensional fluorescent specimens," *J. Opt. Soc. of Am. A* **23**, 1699-1707 (2006).
4. J. Rosen, G. Indebetouw, and G. Brooker, "Homodyne scanning holography," *Opt. Express* **14**, 4280-4285 (2006).
5. J. Rosen and G. Brooker "Digital spatially incoherent Fresnel holography," To be published in *Opt. Lett.*
6. I. Yamaguchi and T. Zhang, "Phase-shifting digital holography," *Opt. Lett.* **22**, 1268-1269 (1997).
7. G. Indebetouw and P. Klysubun, "Spatiotemporal digital microholography," *J. Opt. Soc. of Am. A* **18**, 319-325 (2001).
8. J. Goodman, *Introduction to Fourier Optics*, 2nd ed. (McGraw-Hill, New York, 1996) 63-95.

1. Introduction

Fluorescence is one of the most widely used techniques in many areas of biology, material science and medical imaging because of its sensitivity, selectivity, low background and high contrast. Integration of holography into fluorescence three dimensional (3D) imaging has been difficult because holography requires coherent light and fluorescence emissions are incoherent. Non-fluorescent holography is a well established technique in which holograms are recorded by interfering two mutually coherent beams [1]. This technique cannot be applied to the incoherent light which is characteristic of the emitted light in a fluorescent object. Until now, scanning fluorescence holography [2-4], has been the only way to capture and create a hologram of the incoherent fluorescent emission from the emitted fluorescent

light in 3D structures of an object. In scanning holography, a Fresnel Zone Plate (FZP) pattern from a coherent fluorescence excitation source scans the fluorescent labeled object such that at each and every scanning position the emitted light intensity is integrated by a detector. Since the mechanical scanning process is relatively slow, sensitive to vibration, requires a complex and expensive optical setup to create a FZP from the interference of two coherent beams, we believe it is advantageous to propose an alternative simpler method for fluorescence holography which is free of these drawbacks and has the promise of better performance.

Recently, we have proposed a new method of incoherent digital holography [5] coined FINCH as an acronym for Fresnel INcoherent Correlation Holography. By this method, light is reflected from a 3D object, propagates through or is reflected from a diffractive optical element (DOE) and is recorded by a digital camera. Each beam which originates from any object point is split into two different, mutually coherent, spherical waves. The beam splitting is done by the DOE grating, which operates as if it was a composition of two different diffractive spherical lenses. Therefore, the single wave-front originated from a point-source is divided by the DOE to two wave-fronts with different quadratic curves that propagate in the same direction. The intensity of the two wave-front interference, originated from the same point source, is accumulated incoherently on the camera pixel array with the other interferences from the entire object points to yield the complete hologram. In order to get rid of the twin image and the bias beam resulting from each single hologram which will be described later, three incoherent holograms are recorded sequentially, each with a different phase factor of the DOE. Using the common routines of digital holography [4-6], the three holograms are superposed in the computer, such that the result is a complex valued Fresnel hologram. When this hologram is reconstructed in the computer, a single 3D image of the object appears in the digital reconstruction space. A double channel interferometer with continuous temporal variation of the phase differences between the interfering beams to record non-fluorescent incoherent holograms has been described [7]. This is in contrast to the much simpler motionless single channel FINCH system reported here which has been readily able to produce high quality 3D fluorescent images.

In this study we employ the FINCH technique for color fluorescence imaging. The proposed system produces a color Fresnel hologram which reconstructs the 3D object with its original fluorescent colors. The dice objects in our demonstration contain several spots of two fluorescent dyes each with different emission wavelengths. The objects are illuminated by an arc lamp source with a bandpass filter to illuminate the specimen with incoherent light of about 50 nm bandwidth and which can also excite fluorescence in each of the fluorescent dyes. Several digital holograms are generated for each of the different fluorescent colors on the dice and for the dice themselves. Each emission color is introduced into the recording system by restricting the emission with a specific chromatic filter. For each wavelength of the fluorescence emission and the reflected non-fluorescent light image of the object, a different Fresnel number is applied to the DOE's grating. For each wavelength, three holograms are sequentially recorded, each with a different phase factor of the DOE's function, such that the overall number of captured holograms for M colors plus the complete reflected non-fluorescent image of the object is $3 \cdot (M+1)$. Every three holograms of the same wavelength are superposed in a certain way such that the result is a complex valued Fresnel hologram of this wavelength. The digital reconstruction from each hologram is added to the rest, yielding a complete color 3D image of the original object. To the best of our knowledge, the demonstrated holograms are the first fluorescence holograms recorded without scanning and the first fluorescence multiwavelength emission color holograms ever recorded.

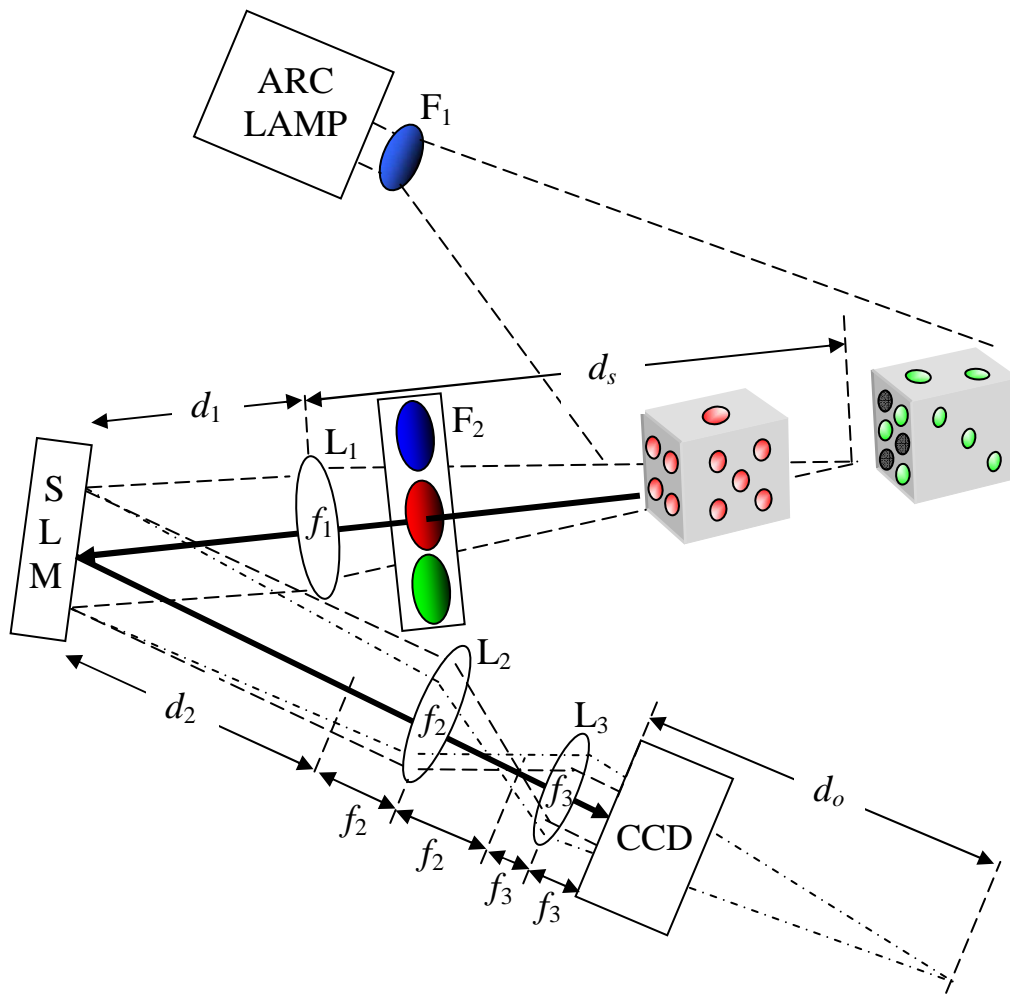


Fig. 1. Schematic of an incoherent digital hologram recorder. SLM: spatial light modulator; CCD: charge-coupled device; L_1 , L_2 , L_3 are spherical lenses and F_1 , F_2 are chromatic filters.

2. Principles of color FINCH

An incoherent blue light source with a bandwidth of 56 nm illuminates a 3D object as is shown in Fig. 1. The object's fluorescent emission light is introduced into the system after passing through one of the chromatic filters F_2 . After passing through lens L_1 , the beam is reflected from a spatial light modulator (SLM) toward a demagnification setup of two lenses L_2 and L_3 , which projects the holographic pattern onto a CCD camera. To understand the operational principle, we analyzed the system by following its response to an input object of a single infinitesimal point. Knowing the system's point spread function (PSF), enables one to analyze the system operation for any general object. In the following analysis, the light is considered as quasi-monochromatic. Such assumption is valid under the condition that the maximal optical path difference between the interfering beams in the system is smaller than the coherence length which is inversely proportional to the spectral bandwidth of the light

source. This condition is well maintained in our single channel on-axis holographic system. A Fresnel hologram of a point object is obtained when the two interfering beams are, for instance, plane and spherical beams. Therefore, we choose the DOE's reflection function $R(x_D, y_D)$ displayed on the SLM to be of the form,

$$R(x_D, y_D) = \frac{1}{2} + \frac{1}{2} \exp \left[-\frac{i\pi}{\lambda a} (x_D^2 + y_D^2) - i\theta \right], \quad (1)$$

where λ is the central wavelength introduced to the system. The constant term of $\frac{1}{2}$ in Eq. (1) contributes the plane wave, and the quadratic phase term is the paraxial approximation of the spherical wave. The angle θ is the phase shift needed in order to get rid of the twin image and the bias term.

The reflection function of the DOE given by Eq. (1) implies that the system's outcome can be viewed as a sum of two overlapping imaging systems. Finding the location of each image is a key concept for understanding this holographic recorder. In one system, let's call it system A, the DOE is actually a converging diffractive lens with a focal length of a , whereas in the other system (system B) the DOE serves as a plane mirror. In system A, a point source located at a distance $d_s = f_1$ from the lens L_1 is imaged to an image point at a distance $(a - d_2)(f_3/f_2)^2$ beyond the camera plane. In this last expression we use the well-known fact that the axial magnification of an ordinary imaging system is given by the relation $M_A = M_T^2 = (d_o/d_s)^2$, where M_T is the transverse magnification, and d_o is the distance from the output aperture to the image. For any point at $(0, 0, z_s)$ located a distance $d_s = f_1 - z_s$ from the lens L_1 , assuming that $z_s \ll f_1$, the distance d_o is approximately,

$$\begin{aligned} d_o(z_s) &\cong (a - d_2) \left(\frac{f_3}{f_2} \right)^2 + \bar{M}_A z_s = (a - d_2) \left(\frac{f_3}{f_2} \right)^2 + \left(\frac{f_3 a}{f_2 f_1} \right)^2 z_s \\ &= \left[\left(\frac{r^2}{f_1 \lambda N} \right)^2 z_s + \frac{r^2}{\lambda N} - d_2 \right] \left(\frac{f_3}{f_2} \right)^2, \end{aligned} \quad (2)$$

where the overall axial magnification \bar{M}_A is the product of magnifications of the two consecutive imaging systems, r is the DOE's radius and N is the DOE's Fresnel number given by $N = r^2/\lambda a$.

In system B, assuming that $d_s \approx f_1$, the object point is obtained far beyond the camera plane at a distance that justifies approximating the location of the image point at infinity. Therefore, for a point at (x_s, y_s, z_s) , the intensity on the camera plane is the square magnitude of the complex amplitude sum of the spherical wave converging at the distance d_o beyond the CCD plane, together with a plane wave, as follows,

$$I_P(x, y) \cong C \left| 1 + \exp \left\{ \frac{-i\pi}{\lambda d_o(z_s)} \left[(x - \bar{M}_T x_s)^2 + (y - \bar{M}_T y_s)^2 \right] - i\theta \right\} \right|^2, \quad (3)$$

where the overall transverse magnification is $\bar{M}_T = f_3 a / f_2 f_1 = f_3 r^2 / \lambda N f_2 f_1$. For a 3D object with intensity distribution $g(x_s, y_s, z_s)$, illuminated by a narrowband incoherent illumination, the intensity of the recorded hologram is an integral over the entire PSFs, given by Eq. (3), over all the object points, as follows

$$H(x, y) = A \left(C' + \iiint g(x_s, y_s, z_s) \exp \left\{ \frac{i\pi}{\lambda d_o(z_s)} \left[(x - \bar{M}_T x_s)^2 + (y - \bar{M}_T y_s)^2 \right] + i\theta \right\} dx_s dy_s dz_s \right. \\ \left. + \iiint g(x_s, y_s, z_s) \exp \left\{ \frac{-i\pi}{\lambda d_o(z_s)} \left[(x - \bar{M}_T x_s)^2 + (y - \bar{M}_T y_s)^2 \right] - i\theta \right\} dx_s dy_s dz_s \right). \quad (4)$$

Besides a constant term C' , Eq. (4) contains two terms of correlation between an object and a quadratic phase, z_s -dependent, function, which means that the recorded hologram is indeed a Fresnel hologram. In order to remain with a single correlation term out of the three terms given in Eq. (4), we follow the procedure of on-axis digital holography [4, 5]. Three holograms of the same object are recorded each of which with a different phase constant θ . The final hologram H_F is a superposition according to the following,

$$H_F(x, y) = H_1(x, y) [\exp(-i\theta_3) - \exp(-i\theta_2)] + H_2(x, y) [\exp(-i\theta_1) - \exp(-i\theta_3)] \\ + H_3(x, y) [\exp(-i\theta_2) - \exp(-i\theta_1)], \\ = \iiint g(x_s, y_s, z_s) \exp \left\{ \frac{i\pi}{\lambda d_o(z_s)} \left[(x - \bar{M}_T x_s)^2 + (y - \bar{M}_T y_s)^2 \right] \right\} dx_s dy_s dz_s, \quad (5)$$

where H_k is the k -th recorded hologram with the phase constant θ_k and $k=1,2,3$.

A 3D image can be digitally reconstructed from $H_F(x, y)$ by calculating the Fresnel propagation [8]. The reconstruction results of different chromatic holograms are composed together to a complete color figure. In order to get the same transverse and axial magnifications for all the wavelengths we change the Fresnel number of the DOE such that $d_o(z_s)$, given by Eq. (2), remains the same for all recorded wavelengths. In other words, the Fresnel number of the $(i+1)$ -th wavelength λ_{i+1} is $N_{i+1} = N_i \lambda_i / \lambda_{i+1}$, where N_i is the Fresnel number of the i -th wavelength λ_i .

3. Experimental results

An experiment showing the recording of a color fluorescence hologram was carried out on the system shown in Fig. 1. The SLM (Holoeye HEO 1080P) is phase-only, and as so, the desired function given by Eq. (1) cannot be directly displayed on this SLM. Instead, as a good approximation for Eq. (1), we chose to display the required quadratic phase function on only half of the SLM pixels. The rest of the pixels were modulated with a constant phase, where the pixels of both types were selected randomly⁵. The small tilt angle of the SLM, from being orthogonal to the optical axis, does not seemingly influence the results. The central 1024×1024 pixels of the SLM, on an area of $9.7\text{mm} \times 9.7\text{mm}$, were used for displaying the DOE. The phase constants of $\theta_{1,2,3} = 0^\circ, 120^\circ, 240^\circ$ were introduced into the three quadratic phase functions. The other specifications of the system are: $f_1 = 250\text{mm}$, $f_2 = 150\text{mm}$, $f_3 = 35\text{mm}$, $d_1 = 135\text{mm}$, $d_2 = 206\text{mm}$.

A pair of $8\text{mm} \times 8\text{mm}$ dice (in which some of the dots were painted with either red or green fluorescent paint) were positioned at the vicinity of the rear focal point of lens L_1 . The center of the die with red fluorescent spots and the die with green fluorescent spots were at a distance of 228mm and 260mm from L_1 , respectively. These dice were illuminated with a mercury arc lamp (Zeiss-AttoArc 2, HBO 100W) in which only light with a peak wavelength of 472nm and a full width at half maximum (FWHM) bandwidth of 56nm was allowed to pass through bandpass filter F_1 . All of the holograms were recorded by a cooled CCD camera (Hamamatsu Digital Camera C4742-95, 12 bit, 1024×1280 pixels, bin 1) and processed by a PC. The first three holograms ($0, 120$ and 240 degrees) of the non-fluorescent surfaces on the dice were recorded with an identical filter as the source's filter mentioned above placed in the emission filter slider F_2 . The Fresnel number for these holograms was chosen to be $N_B = 10$ (based upon a center wavelength of 472nm). The magnitude and phase of the final

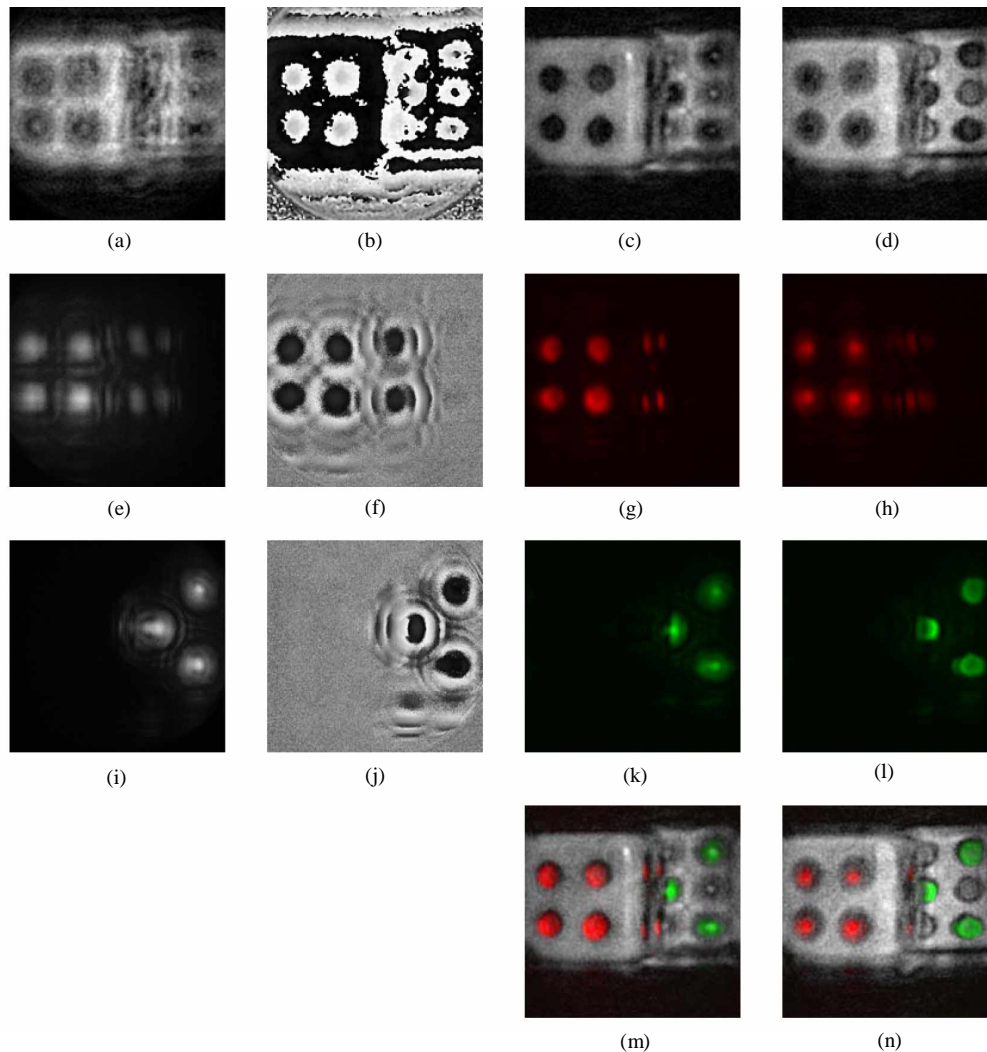


Fig. 2. (a). Magnitude and (b) phase of the complex Fresnel hologram of the dice. Digital reconstruction of the non-fluorescence hologram: (c) at the face of the red-dots on the die, and (d) at the face of the green dots on the die. (e) Magnitude and (f) phase of the complex Fresnel hologram of the red dots. Digital reconstruction of the red fluorescence hologram: (g) at the face of the red-dots on the die, and (h) at the face of the green dots on the die. (i) Magnitude and (j) phase of the complex Fresnel hologram of the green dots. Digital reconstruction of the green fluorescence hologram: (k) at the face of the red-dots on the die, and (l) at the face of the green dots on the die. Compositions of Figs 2(c), 2(g) and 2(k) and Figs 2(d), 2(h) and 2(l) are depicted in Figs. 2(m) and 2(n), respectively.

complex hologram, superposed from the first three holograms, are shown in Figs. 2(a) and 2(b), respectively. The reconstruction from the final hologram was calculated using the Fresnel propagation formula [8]. The results are shown at the plane of the front face of the front die in Fig. 2(c), and at the plane of the front face of the rear die in Fig. 2(d). Note that in each plane a different die face is in focus as is indeed expected from a holographic reconstruction of an object with a volume. The second set of three holograms was recorded via a red filter in the emission filter slider F_2 which passed fluorescent light with a peak wavelength of 626 nm and FWHM bandwidth of 11 nm. The Fresnel number during the

recording of the 'red' holograms was $N_R=7.8$. The magnitude and phase of the final complex hologram, superposed from the 'red' set, are shown in Figs. 2(e) and 2(f), respectively. The reconstruction results from this final hologram are shown in Figs. 2(g) and 2(h) at the same planes as in Figs. 2(c) and 2(d), respectively. Finally, an additional set of three holograms was recorded with a green filter in emission filter slider F_2 which passed fluorescent light with a peak wavelength of 516 nm and FWHM bandwidth of 16 nm. The Fresnel number during the recording of the 'green' holograms was $N_G=9.2$. The magnitude and phase of the final complex hologram, superposed from the 'green' set, are shown in Figs. 2(i) and 2(j), respectively. The reconstruction results from this final hologram are shown in Figs. 2(k) and 2(l) at the same planes as in Figs. 2(c) and 2(d), respectively. Compositions of Figs. 2(c), 2(g) and 2(k) and Figs. 2(d), 2(h) and 2(l) are depicted in Figs. 2(m) and 2(n), respectively. Note that all the colors in Fig. 2 are pseudo-colors. These last results yield a complete color 3D holographic image of the object including the red and green fluorescence. While the optical arrangement in this demonstration has not been optimized for maximum resolution, it is important to recognize that even with this simple optical arrangement, the resolution is good enough to image the fluorescent emissions with good fidelity and to obtain good reflected light images of the dice. Furthermore, in the reflected light images in Figs. 2(c) and 2(m) the system has been able to detect a specular reflection of the illumination from the upper right corner of the front dice.

4. Conclusions

In conclusion, we have proposed and demonstrated a process of recording color holograms of 3D fluorescent objects. This motionless system does not require complicated alignment or a laser and the bandwidth can be wider than conventional incoherent interferometers, entirely because this holographic recorder is implemented on a single channel setup. The proposed design might play an important role in many types of 3D fluorescence applications including fluorescence microscopy so that multicolor 3D structures and dynamic processes could be imaged without any scanning, and therefore would be expected to be faster than other methods.